COMSOL
CONFERENCE
2023 MUNICH

Modelling of convective heat and moisture transfer in porous bulk insulation for large-scale thermal energy storage

A. Tosatto[1], F. Ochs[1], M. Bianchi Janetti[1]
1. Unit of Energy Efficient Buildings, Department of Structural Engineering and Material Sciences, Universität Innsbruck, Innsbruck, Austria.

Abstract
The utilization of thermal energy storage (TES) systems is pivotal in the context of energy systems reliant on fluctuating renewable sources. To enhance TES system efficiency within specific cost limits, design considerations must encompass operational traits and envelope material properties. Challenges arise due to the required installation ease and affordability, limiting insulation material options. The occurrence of elevated moisture (up to 100% RH) and temperatures (around 90/95 °C) necessitates understanding the material behavior in this temperature and moisture range. Viable materials are mineral- or rockwool, foam glass gravel, expanded glass, and perlite. However, heat flow direction (upward for covers, horizontal for side walls) and open porosity can trigger convective heat and mass transfer, increasing thermal losses. Infiltration risks and accumulated moisture degrade the insulation, enhancing the heat transfer.
Investigating similar real-application boundary conditions is essential for multiphysical assessment. This study employs experimental characterization and numerical simulations, using Comsol Multiphysics, to predict the material behavior and define properties. A mock-up of the TES cover insulation, including a heating plate simulating operational conditions, is set up to give a reference for the numerical model. The case of compacted foam glass gravel is analysed. Initial dry condition analysis encompasses conductive and convective heat transfer, coupled with fluid flow in porous media. Moisture influence is explored in a subsequent phase, integrating a moisture transport equation. The validated model aids further developments to inhibit natural convection effects or minimize their impact.
Keywords: Thermal energy storage, porous insulation, natural convection, moisture transport, numerical modelling

Introduction
The application of large-scale water-based thermal energy storages (TES) has seen a rapid increase in the last decades in Europe and China [1]. They enable to increase the renewables fraction in district heating grids, as they allow to store the surplus of energy both on daily and seasonal basis. A challenge often observed during their operation is however related to the performance of the insulation, which is required to limit the thermal losses towards the surroundings. The need for ease and low cost limits the choice of insulation materials that can be considered. Moreover, the presence of high moisture contents and temperatures (water is stored at a temperature of 90/95 °C) requires an in-depth knowledge of the material behavior. Possible materials that are considered suitable for this application are either mineral- (MW) or rockwool (RW) or foam glass gravel (FGG), expanded glass (EG) and perlite [2][3].
The presence of open porosity within the insulation and the high temperature gradients can lead to the development of convective heat transfer alongside conduction and radiation, thus increasing the thermal losses [4]. This phenomenon is particularly critical in presence of an upwards heat flux, as in the case of the TES cover, which separates the high temperature upper water layers from the external air.
Another source of increased heat losses is represented by the presence of moisture in the insulation. Residual moisture can be present within the insulation at the end of the construction phase. Moreover, there is a risk of water and vapour infiltrations both from the TES (diffusion through the liner and leakages) and from rainfall, thus leading to the accumulation of moisture within the insulation layer [5].
The planner faces thus a multiphysical problem, which combines the radiative and conductive heat transfer, with the convective transfer related to the variation of the fluid density within the bulk insulation. The third essential element is represented by the presence of moisture.

Theory
In dry, solid materials, heat transfer is primarily related to the conductive and radiative heat transfer, driven by the temperature difference and the characteristics of the material itself (i.e., the effective thermal conductivity λ). In porous materials, however, the heat transfer can be further enhanced by convection (in this case air convection), which in the TES envelope is driven primarily by buoyancy forces. Temperature gradients within the bulk determine local variations of the air density (ρ), thus establishing gravitational body forces proportional to the density of the air [6].

Alongside the energy balance equation (Eq. 1), it is therefore necessary to introduce the momentum equation (Eq. 2), in order to solve the velocity field of the fluid. In this specific case, the Brinkman equation appears to be the most suitable approach, as it enables modelling the momentum transport in porous media.
In presence of moisture, an additional term, linked to the transfer of latent heat, must be added to the energy balance equation, thus requiring the introduction of a 3rd equation to solve the moisture transfer (Eq. 3).

$$\left(\rho C_p\right)_{eq}\frac{\partial T}{\partial t} = \nabla\cdot\left(\lambda_{eq}\nabla T\right) - \left(\rho C_p\right)_{eq} u\cdot\nabla T + \nabla\cdot\left(L_v\left(\frac{D_{av}}{RT\mu_{diff}}\right)\nabla(\varphi\, p_{sat})\right) \quad (1)$$

$$\rho\frac{du}{dt} = \nabla\cdot\left[-pI + \frac{\eta}{\psi}(\nabla u + (\nabla u)^T) + \frac{2}{3}\frac{\eta}{\psi}(\nabla u)I\right] + \rho g\beta(T - T_c) + \frac{\eta}{K}u \quad (2)$$

$$\frac{\partial w}{\partial t} + u\cdot\nabla w = -\nabla\cdot\left(\frac{\mathrm{D_{av}}}{\mathrm{RT}\mu_{\mathrm{diff}}}\nabla(\varphi\, p_{sat})\right) \quad (3)$$

Experimental Set Up

In order to calibrate the implemented model and to determine the missing material properties, an experimental set up was built in the climate chamber of the University of Innsbruck. The mock-up consists of a (1x1x0.5) m container filled with bulk insulation (FGG), see Figure 1. In order to simulate the specific condition of the TES cover, a heating plate was placed on the bottom of the container, to reach a constant temperature of 60 °C. Most favorable conditions for the development of convective heat (and mass) transfer are therefore realized. The lateral walls are insulated with high performance insulation panels (vacuum insulation panels, VIP) to ensure adiabatic boundary conditions.

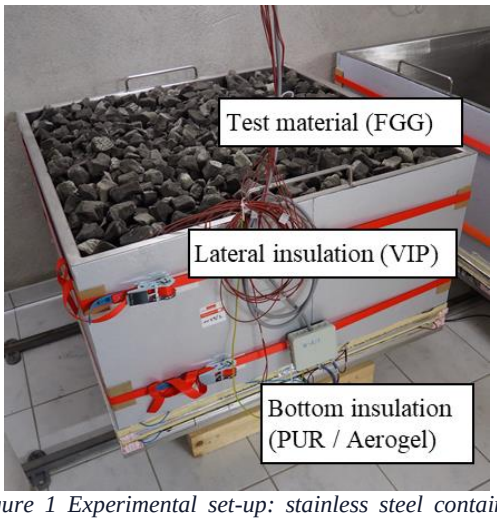

Figure 1 Experimental set-up: stainless steel container with lateral insulation (vacuum insulation panel).

The compaction of the material was achieved with three compaction steps, in order to realize a relatively homogeneous degree of compaction (30 %).
Six temperature sensors (Pt100) are installed in the insulation domain: 3 in the central part and 3 nearby the border, distributed along the vertical (Figure 2).

Research question

In this study, the challenges concerning the validation of the numerical model are tackled. In particular, the influence of the variation of the material parameters (primarily the permeability) on the fluid velocity field and thereby on the temperature distribution is investigated.
Another important aspect analyzed in the paper concerns the challenge of extending the results of the test to the real application. While the experimental set up is necessarily of limited size (1 m^2 surface), the real application will see far larger surfaces (>1000 m^2). The impact of the border effects is therefore investigated to suggest eventual improved implementations of the experiment.

Implementation in COMSOL Multiphysics

In order to model the experimental mock-up, Equations (1), (2) and (3) are implemented in COMSOL Multiphysics to simulate the heat transfer, the fluid flow and the moisture transport in the insulation. At this purpose, the modules *Heat Transfer in Porous media*, *Brinkman Equations* and *Moisture Transport in Building Materials* are applied.
In dry conditions, energy balance equation and Brinkman equation are sufficient.

$$\left(\rho C_p\right)_{eq}\frac{\partial T}{\partial t} = \nabla\cdot\left(\lambda_{eq}\nabla T\right) - \left(\rho C_p\right)_{eq} u\cdot\nabla T \quad (4)$$

$$\rho\frac{du}{dt} = \nabla\cdot\left[-pI + \frac{\eta}{\psi}(\nabla u + (\nabla u)^T) + \frac{2}{3}\frac{\eta}{\psi}(\nabla u)I\right] + \rho g\beta(T - T_c) + \frac{\eta}{K}u \quad (5)$$

These equations are implemented to study the behavior of the tested insulation material. For the container and insulation layers the simple *Heat Transfer in Solids* module is applied.
As reference, a simplified model using the only *Heat Transfer in Solids* module is additionally implemented, in order to assess the relevance of convective over conductive heat transfer. In this model, the influence of convection is introduced through the Nusselt number, which expresses the ratio of convection to pure conduction [6]:

$$h = \frac{Nu\,\lambda}{\Delta x} \quad (6)$$

Therefore, Equation (4) becomes:

$$(\rho C_p)_{eq}\frac{\partial T}{\partial t} = \nabla\cdot(\lambda_{eq} Nu\,\nabla T) \quad (7)$$

where the effective thermal conductivity ($\lambda_{eq}Nu$) considers the combined effect of radiative, conductive and convective heat transfer, without the need for the momentum equation. This implementation, however, does not allow to investigate local buoyancy effects. It is important to highlight that the Nusselt number does not only depend on the material characteristics, but also on the specific operation conditions, such as temperature difference and sample thickness. In order to reduce the simulation time, this simplified model is considered in a second step also for investigation of the relative humidity distribution within the insulation.
Table 1 presents the parameters used in the simulation for the studied material.

Table 1 Material Properties used in the simulation..

Insulation material (i.e. compacted FGG)		
thermal conductivity, λ	0.1	[W/(m·K)]
density, ρ	190	[kg/m^3]
heat capacity, c_p	1000	[J/(kg·K)]
free saturation water content, u_{fs}	300	[kg/m^3]
permeability, K	$2\cdot10^{-7}$ to $7\cdot10^{-7}$	[m^2]

In absence of manufacturer data concerning the permeability of a FGG bulk, a parameter analysis is conducted. According to a previous work [4], a range of permeability between K=$15\cdot10^{-7}$ m^2 and K=$3\cdot10^{-7}$ m^2 is assumed, depending on the degree of compaction. The simulated results are then compared with the measurements to identify the permeability range for the analysed material.
Figure 2 shows a sketch of the model implemented in COMSOL. Considering the presence of a guarded heating plate, the bottom is assumed to be adiabatic, while two conditions are investigated for the lateral wall, one adiabatic and one with a convective heat flux boundary condition (with h=10 W/(m^2·K)). The top of the sample is considered as an open boundary with heat flux boundary conditions (with h=10 W/(m^2·K)).
In order to simplify the problem and reduce the computational time, a 2D model is implemented, exploiting the symmetry of the sample (see Figure 1). The temperature sensors position of the experimental set-up is replicated in COMSOL using *Point Probes*.

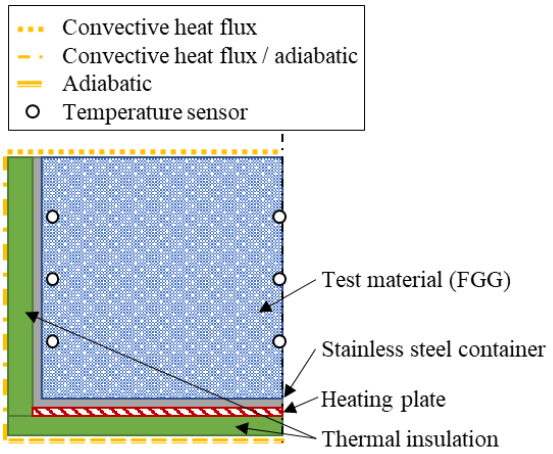

Figure 2 Sketch of the central section of the sample as modelled in COMSOL with studied boundary conditions.

Although the measurement conditions are stationary, a time dependent study is carried out, using the fully coupled approach, to reach convergence. The power of the heating plate is defined in the model using the *Boundary Heat Source Tool*; the power input of the experimental set up to maintain a temperature of 60 °C is used. The average temperature of the climate chamber is 19.5 °C.

Results and Discussion

Dry conditions

The comparison between simulated and measured temperatures is presented in Figure 3 (central sensors) and Figure 4 (lateral sensors).
From the simplified *Solid domain study*, the best matching is achieved with a Nusselt number Nu=2 [5], indicating that the impact of convection is not negligible. However, the simulated temperature profile obtained with this simplified approach shows major deviations from the measured data.
The gray lines represent the temperature profiles obtained by numerical simulation with the Brinkman equation, applying different permeabilities. The best match between simulation and measured outcomes is obtained for K=$2\cdot10^{-7}$ m^2, in agreement with the data available from the literature. Some deviation is observed on the lower part of the tank, which is reasonably explained by the fact that the lower layer may have a higher compaction degree.

The red lines represent the temperature profile in presence of adiabatic conditions: as expected, same permeability values would result in higher temperatures.
The influence of multiphysics is particularly evident closer to the border (Figure 4), where the measured temperatures are significantly lower than the ones simulated with the simplified adiabatic approach.

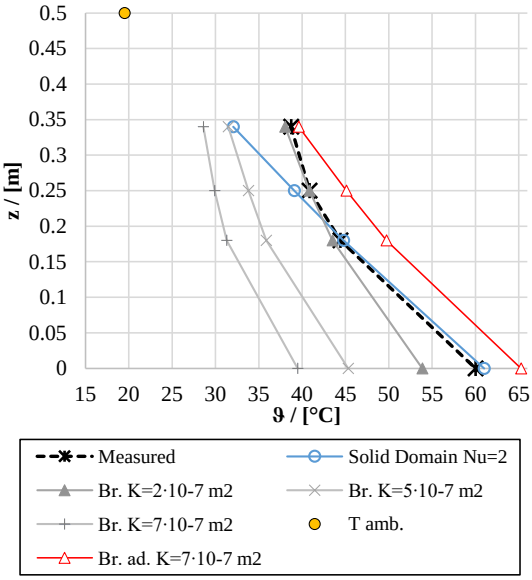

Figure 3 Vertical temperature profile on the central part of the studied insulation according to the measurements and to the numerical simulations (Br: with Brinkman model, Br. ad.: Brinkman model with adiabatic boundary conditions).

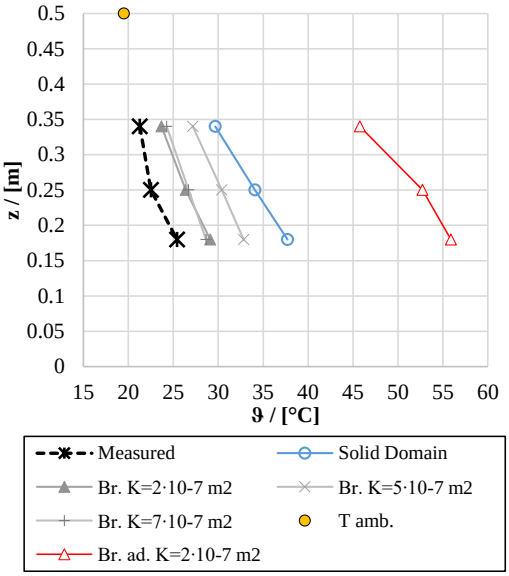

Figure 4 Temperature near the border of the studied insulation according to the measurements and to the numerical simulations (Br: with Brinkman model, Br. ad.: Brinkman model with adiabatic boundary conditions).

The influence of buoyancy flow development on the temperature distribution within the experimental set-up is presented in Figure 5 (considering lateral losses) and Figure 6 (for ideal lateral adiabatic conditions).

It can be observed that the colder air of the upper layers flows down, and rises in the central part of the sample, once its temperature increases in the lower warmer layers.
The permeability appears to have an influence on the shape of the buoyant plume. Higher permeabilities are associated with higher mixing, thus resulting in lower temperatures.

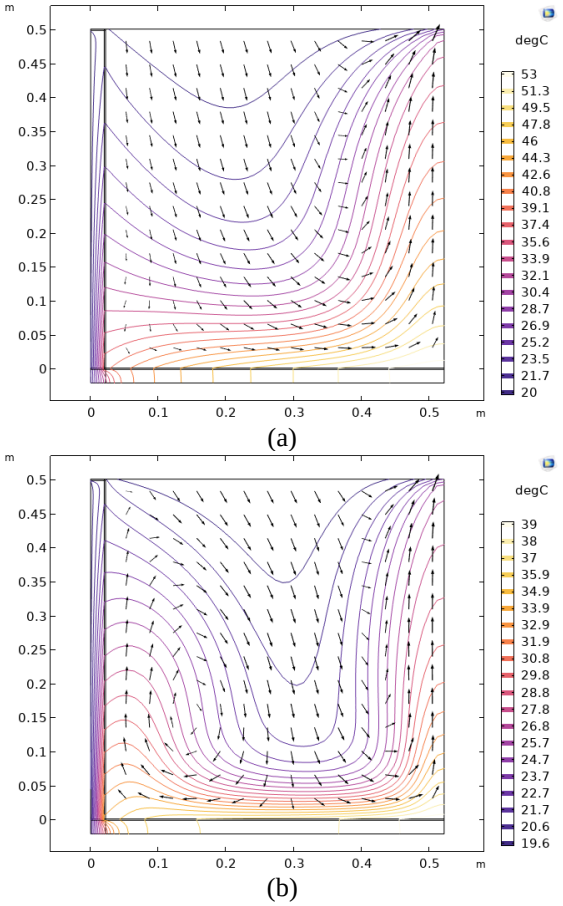

Figure 5 Temperature contour plot and velocity field for the case with realistic boundary conditions (a) $K=2\cdot10^{-7}$ (b) $K=7\cdot10^{-7}$.

An interesting comparison can be made observing Figure 5(a) and Figure 6(a), both obtained with a permeability value $K==2\cdot10^{-7}$ m^2. The presence of adiabatic boundary conditions results in variations of the horizontal temperature variations. The high impact of boundary conditions on the buoyancy plume and on the isotherms profile suggests that these need to be taken into account when extending the analysis to the real conditions that can occur in a wide TES cover. This suggests the possibility of the development of local buoyant plumes, that make the heat transfer within the bulk highly unstable, as previously highlighted in [3].

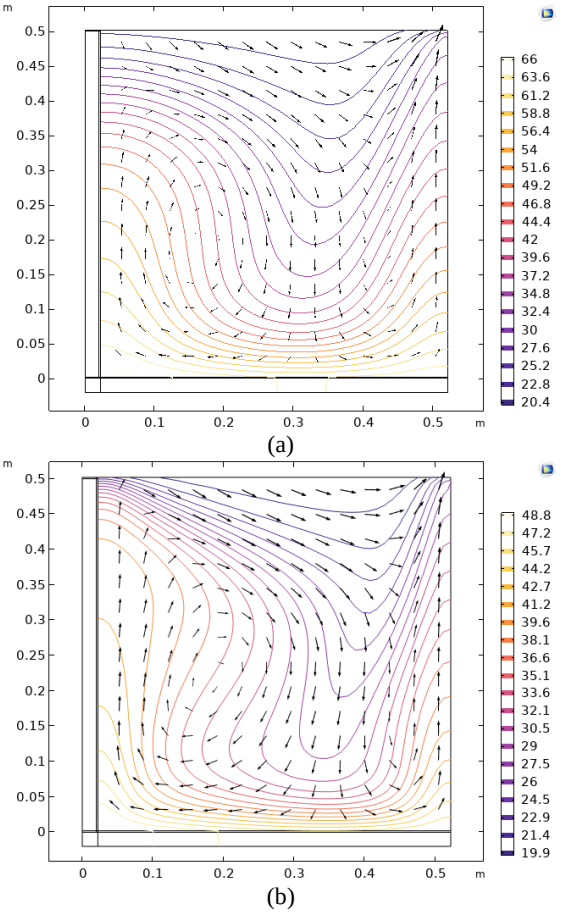

Figure 6 Temperature contour plot and velocity field for the case with adiabatic boundary conditions (a) $K=2\cdot10^{-7}$ (b) $K=7\cdot10^{-7}$.

Moist conditions

As highlighted by dry tests and numerical simulations, in bulk materials like FGG the (natural) convection plays a significant role. This extends also to the moist conditions. Due to diffusion through the liner or leakages, the moisture content within the material can increase and its transport is not only related to diffusion but also to convection, according to Equation (2). The temperature gradient within the insulation layer results in an uneven distribution of the relative humidity with possible saturation in the upper insulation layers. This may lead to water condensation on the top and to a challenging removal of the trapped moisture.

In this last section we investigate this condensation risk. In order to simulate what could happen in a section of a TES cover, adiabatic lateral conditions are considered. As in the previous section, the analysed material is compacted FGG.

In order to estimate the impact of convective mass transfer, 10 liters of water are sprayed on the specimen (Figure 1), and the drying profile of the material is obtained by measuring the gradual weight loss due to the water evaporation. In this analysis, the simplified heat transfer equation using the Nusselt number to represent the impact of convection is implemented, with the moisture transport equation including an effective water vapor diffusion resistance factor (μ_{eff}) to consider the role of convection. In absence of data for the FGG water storage function, the one suggested in [5] is used. The effective water resistance factor of the material is then derived though comparison to the simulation results. A comprehensive description of this study is presented in [5]. The comparison between simulated and measured data for the investigated sample is presented in Figure 7.

The resulting value of effective water vapor resistance is lower than 1; this result is attributable to the convective component, which is included in μ_{eff}, meaning that the drying of the material is primarily driven by convection, while diffusion plays a minor role.

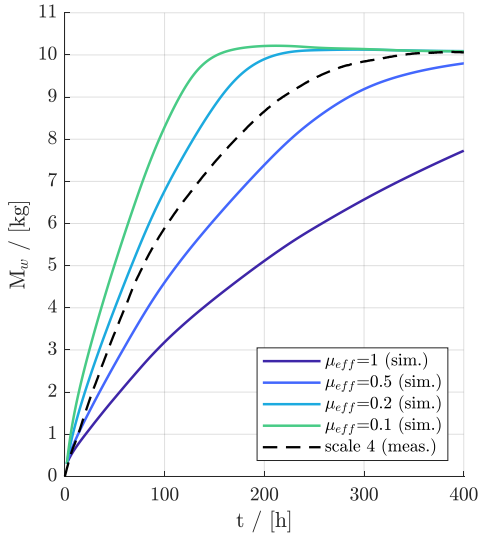

Figure 7 Comparison between simulated (continuous lines) and measured (black dashed line) drying curves [5].

This result is used for further investigating the hygrothermal behavior of a TES cover during its operation. With respect to the experimental model presented in the previous section, where a constant power input is given as boundary condition, a constant temperature is here assumed on the top (20 °C) and bottom (60 °C) of the insulation. Additionally, it is assumed that for an entire year, an amount of 5 g/(m^2·day) of water is able to diffuse through the bottom liner (starting from an initial relative humidity of 50 %). The upper layer of the cover is assumed impermeable.

Figure 8 shows the vertical temperature profile, the relative humidity distribution and moisture content in a 50 cm compacted FGG. It is possible to observe that, while the additional moisture content is not significant (ca. 1.8 kg/(m^2·a)), the final temperature distribution leads to high relative humidity values and moisture content on the top.

Given the relevance of convective heat transfer observed in the analysis of dry conditions, it is important to remark the fact that the simplified model without momentum equation is not able to predict the real temperature distribution. The curves presented in Figure 8 are meant as a starting point for

further analysis of heat and moisture transfer in porous media with high temperature differences.

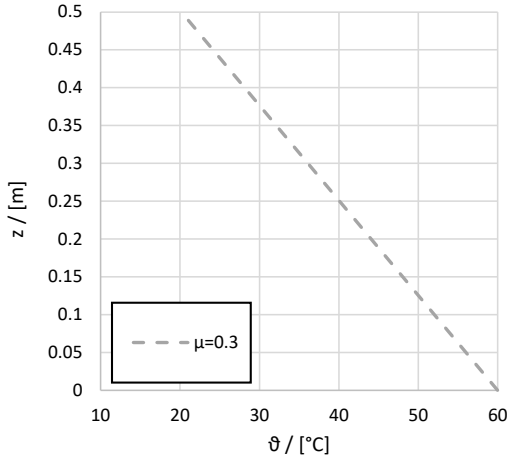

(a)

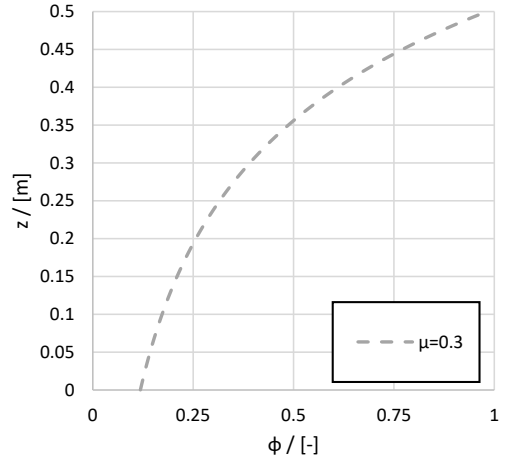

(b)

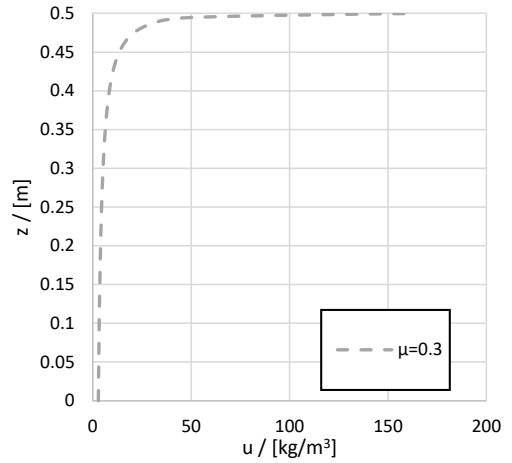

(c)

Figure 8 (a) Vertical temperature profile, (b) relative humidity distribution and (c) moisture content at the end of the year.

Conclusions

Finite element-based numerical simulation are a powerful source of information to establish the behavior of insulation materials and to account for the different phenomena that may occur.

In the study of insulation material for buried TES, this aspect becomes particularly relevant considering the lifetime of the installations. A frequent replacement of insulation because of its degradation is not economically feasible; therefore, a planning of effective solutions for moisture removal is necessary.

The comparison between numerical and measured data allowed to validate a numerical model that can be implemented to study effective measures useful for the practice. Further development of the numerical model should take into account the influence of convective moisture transfer on the final humidity distribution.

Nomenclature

Symbol	Description
Latin Symbols	
C_p	specific heat capacity / [J/(kg·K)]
D_{av}	vapour diffusivity in air/ [m^2/s]
g	gravitational acceleration / [m/s^2]
h	heat transfer coefficient / [W/(m^2·K)]
I	Identity matrix
K	permeability / [m/s]
L_v	latent heat / [J/kg]
M	mass / [kg]
p	pressure / [Pa]
R	gas constant / [J/(kg·K)]
T	temperature / [K]
t	time / [s]
u	velocity / [m/s]
w	specific water content / [kg/m^3]
x	horizontal coordinate / [m]
z	vertical coordinate / [m]
Greek Symbols	
β	Volumetric thermal expansion coefficient / [K^{-1}]
η	dynamic viscosity / [Pa·s]
ϑ	temperature / [°C]
λ	thermal conductivity / [W/(m·K)]
μ	water vapour diffusion resistance factor / [-]
ρ	density / [kg/m^3]
φ	relative humidity / [%]
ψ	porosity
Subscripts	
a	air
eq	equivalent
ins	insulation
m	mass
sat	saturation
v	vapour

References

[1] D. Tschopp, Z. Tian, M. Berberich, J. Fan, B. Perers, and S. Furbo, “Large-scale solar thermal systems in leading countries: A review and comparative study of Denmark, China, Germany and Austria,” *Appl. Energy*, vol. 270, p. 114997, Jul. 2020, doi: 10.1016/j.apenergy.2020.114997.

[2] F. Ochs, “Modelling Large-Scale Thermal Energy Stores,” University of Stuttgart, 2009.

[3] F. Ochs, M. Bianchi, and J. Ondrej Klesnil, “Wärmeleitfähigkeit von Schüttungen aus Glasschaumgranulat: Messtechnische Analyse sowie Analytische und Numerische Modellierung,” 2015. [Online]. Available: http://www.aee-now.at/cms/fileadmin/downloads/projekte/store4grid/store4Grid Wärmeleitfähigkeit.pdf.

[4] M. Bianchi Janetti, T. Plaz, F. Ochs, O. Klesnil, and W. Feist, “Thermal conductivity of foam glass gravels: A comparison between experimental data and numerical results,” in *6th Int. Build. Phys. Conf. IBPC 2015, Torino, Italy*, 2015, vol. 78, pp. 3258–3263, doi: 10.1016/j.egypro.2015.11.713.

[5] A. Tosatto, F. Ochs, A. Dahash, C. Muser, F. Kutscha-Lissberg, and P. Kremnitzer, “Influence of Heat and Mass Transfer on the Performance of Large-Scale Thermal Energy Storage Systems,” in *Proceedings of the International Renewable Energy Storage Conference (IRES 2022)*, 2023, pp. 470–488, doi: 10.2991/978-94-6463-156-2_30.

[6] F. P. Incropera, D. P. Dewitt, T. L. Bergman, and A. S. Lavine, *Incropera’s Principles of Heat and Mass Transfer*, Global Edi. Wiley, 2017.

Acknowledgements

This research was carried out within the framework of the research project “ScaleUp4TESins” (“Wissenschaftliche Untersuchungen zu Dämmstoffschüttungen”) and IEA ECES Annex 39 (“Großwärmespeicher für Fernwärmesysteme”, Project Nr: 883015). Therefore, the authors wish to acknowledge the financial support for this work.